


BRIEF DEFINITIVE REPORT

Chronic TREM2 activation exacerbates A β -associated tau seeding and spreading

Nimansha Jain^{1,2,3} , Caroline A. Lewis^{1,2,3} , Jason D. Ulrich^{1,2,3} , and David M. Holtzman^{1,2,3} 

Variants in the triggering receptor expressed on myeloid cells 2 (*TREM2*) gene are associated with increased risk for late-onset AD. Genetic loss of or decreased *TREM2* function impairs the microglial response to amyloid- β (A β) plaques, resulting in more diffuse A β plaques and increased peri-plaque neuritic dystrophy and AD-tau seeding. Thus, microglia and *TREM2* are at a critical intersection of A β and tau pathologies in AD. Since genetically decreasing *TREM2* function increases A β -induced tau seeding, we hypothesized that chronically increasing *TREM2* signaling would decrease amyloid-induced tau-seeding and spreading. Using a mouse model of amyloidosis in which AD-tau is injected into the brain to induce A β -dependent tau seeding/spreading, we found that chronic administration of an activating *TREM2* antibody increases peri-plaque microglial activation but surprisingly increases peri-plaque NP-tau pathology and neuritic dystrophy, without altering A β plaque burden. Our data suggest that sustained microglial activation through *TREM2* that does not result in strong amyloid removal may exacerbate A β -induced tau pathology, which may have important clinical implications.

Introduction

Alzheimer's disease (AD) causes progressive decline in memory and cognitive function which ultimately leads to death. Currently, there is no treatment that effectively slows or stops the progression of AD. Given that this disease affects one in eight Americans over the age of 65, there is a dire need for a better understanding of the underlying pathophysiology to enable development of effective treatment options.

The neuropathological hallmarks of AD include extracellular plaques composed primarily of aggregated amyloid- β (A β) peptides and intraneuronal neurofibrillary tangles containing aggregated, hyperphosphorylated forms of tau protein (p-tau). An important subtype of A β plaques includes neuritic plaques (NPs), which are defined as plaques surrounded with swollen, dystrophic neural processes also containing aggregated p-tau (Holtzman et al., 2011; Nelson et al., 2012). In those with existing A β pathology, the progression of tau pathology into the limbic cortex and neocortex parallels cognitive impairment (Nelson et al., 2012). A β plaques also mediate local tau seeding in dystrophic neurites and contribute to the formation and spread of p-tau in NPs and neurofibrillary tangles in mice (He et al., 2018).

In addition to deposition of protein aggregates, neuroinflammation that includes reactive microglia is a common feature of AD (Ransohoff, 2016). Microglia are the brain-resident

innate immune cells (Domingues et al., 2016). Under normal conditions, microglia and macrophages act in a coordinated manner as the first line of defense against both internal and external insults (Ginhoux and Guillemins, 2016; Netea et al., 2020). In response to pathology and toxic stimuli, microglia change their morphology, antigen presentation, and phagocytic capacity in an attempt to mitigate insults (Butovsky and Weiner, 2018; Ruan et al., 2021). In the human AD brain and in mouse models with A β or tau pathology, a population of microglia has been described as disease-associated microglia (DAM) and a portion of this population clusters around A β plaques. In DAM, there is also down-regulation of the expression of homeostatic microglial genes such as *Tmem119* and *P2ry12*, while there is an increase in the expression of activation-linked markers such as *Clec7a* and *apoE* (Deczkowska et al., 2018; Keren-Shaul et al., 2017). Recent genetic studies have highlighted the central role of innate immunity in neurodegeneration by identifying several risk variants in genes that are exclusively expressed within microglia in the brain. Most notably, rare variants, such as the R47H mutation in the *TREM2* gene, increase risk for late-onset AD two- to four-fold (Guerreiro et al., 2013; Jonsson et al., 2013). *TREM2* is a cell surface receptor expressed specifically by microglia in the brain. The precise ligand(s) that activate *TREM2* in vivo are unclear. Previous in vitro studies suggest that anionic

¹Department of Neurology, Washington University School of Medicine, St. Louis, MO; ²Hope Center for Neurological Disorders, Washington University School of Medicine, St. Louis, MO; ³Knight Alzheimer's Disease Research Center, Washington University School of Medicine, St. Louis, MO.

Correspondence to David M. Holtzman: holtzman@wustl.edu.

© 2022 Jain et al. This article is distributed under the terms of an Attribution-Noncommercial-Share Alike-No Mirror Sites license for the first six months after the publication date (see <http://www.rupress.org/terms/>). After six months it is available under a Creative Commons License (Attribution-Noncommercial-Share Alike 4.0 International license, as described at <https://creativecommons.org/licenses/by-nc-sa/4.0/>).

phospholipids, nucleotides, and also apoE can stimulate TREM2 activity (Atagi et al., 2015; Wang et al., 2015). TREM2 signaling occurs through the immunoreceptor tyrosine-based activation motif-containing adaptor DAPI2 (Lanier et al., 1998; Ulrich et al., 2017). TREM2 signaling supports diverse processes such as phagocytosis and clustering around debris, increased metabolic function, and lipid metabolism (Cui et al., 2021; Gratuze et al., 2018; Nugent et al., 2020; Ulland et al., 2017).

In regard to the role of TREM2 in AD, recent *in vivo* studies suggest that TREM2 function may be protective or damaging depending on the stage of pathology that is present. In models of A β pathology, TREM2 deficiency or partial loss of function with the R47H TREM2 variant results in decreased microglial clustering and activation around A β plaques, with corresponding greater levels of axonal dystrophy (Colonna and Wang, 2016; Gratuze et al., 2020; Leyns et al., 2019; Yuan et al., 2016). Further, following injection of human AD brain-derived pathological tau (AD-tau) into the brain in amyloid depositing mice with decreased TREM2 function results in increased tau seeding and spreading (Colonna and Wang, 2016; Gratuze et al., 2020, 2021; He et al., 2018; Leyns et al., 2019; Yuan et al., 2016). Also, the removal of microglia using a CSF1R antagonist increased amyloid-associated tau seeding (Gratuze et al., 2021). Together, these results suggest that in the setting of extracellular amyloid, the presence of normal TREM2 function in microglia can suppress A β -induced tau seeding and spreading. There is also evidence that once significant tau pathology is in the brain that results in neurodegeneration, as in models of pure tauopathy, loss of TREM2 decreases tau-mediated neurodegeneration (Leyns et al., 2017; Gratuze et al., 2020).

TREM2 function appears protective during the early phases of AD pathology, suggesting that increasing TREM2 activation above basal levels may be a therapeutic strategy for AD. Several studies that use TREM2-targeted antibodies to stimulate TREM2 activation within amyloid models have shown a variety of potentially beneficial effects on neuroinflammation, A β plaque pathology, microglial function, and neuritic dystrophy (Cheng et al., 2018; Cignarella et al., 2020; Ellwanger et al., 2021; Fassler et al., 2021; Price et al., 2020; Schlepckow et al., 2020; Wang et al., 2020). These results indicate targeting activation of TREM2 and microglia as a therapeutic appears promising and has moved into human clinical trials in AD (Schlepckow et al., 2020; Wang et al., 2020). To further explore whether administration of an activating TREM2 antibody might exert beneficial effects on not just aspects of A β -related pathology but also A β -induced tau seeding and spreading, we tested the effect of an anti-mouse TREM2 agonist antibody, AL002a, in a combined A β and tau model hypothesizing that chronic TREM2 activation would inhibit amyloid-induced tau seeding and spreading.

Results and discussion

Chronic TREM2 agonist antibody administration increases DAM around plaques

To investigate the role of chronic TREM2 agonist antibody administration on amyloid-induced peri-plaque and NP-tau pathology, we used a previously described model of amyloid-

induced tau seeding and spreading by injecting mouse brains with sarkosyl-insoluble tau aggregates isolated from human AD brain tissue (AD-tau; He et al., 2018; Leyns et al., 2019). 6-mo-old 5XFAD mice were injected unilaterally with AD-tau into the dentate gyrus of the hippocampus (HC) and overlying cortex. 1 wk prior to AD-tau injection, these mice began a chronic treatment paradigm in which mice were treated *i.p.* weekly with 80 mg/kg of the murine TREM2 antibody or with 80 mg/kg of a murine IgG control antibody until 9 mo of age (Fig. 1 A). The antibodies were injected 1 wk prior to AD-tau injections to begin the treatment to test how TREM2 agonist would affect amyloid induced tau seeding and spreading prior to the establishment of any tau pathology. We chose a pre-treatment paradigm, as we wanted to mimic what occurs in humans with preclinical AD or the very early stages of mild cognitive impairment due to AD where there is substantial amyloid pathology and where there is still little to no neocortical tau pathology (Long and Holtzman, 2019). This TREM2 antibody has been previously shown to be an agonist and targets the stalk region of TREM2 through *in vitro* and *in vivo* studies (Cignarella et al., 2020; Price et al., 2020). We confirmed higher phosphorylation of syk, the kinase phosphorylated following TREM2 ligand binding, in BMDMs following 3 h of treatment with the TREM2 antibody (Fig. S3 K). We also saw an increase in syk phosphorylation in 9-mo-old 5XFAD mouse cortical samples following two *i.p.* doses of 80 mg/kg of the TREM2 antibody (Fig. S3 K). Additionally, we confirmed robust levels of the TREM2 antibody in terminal plasma (Fig. 1 B) following weekly chronic administration as well as in the plasma and mouse cortical tissue after acute administration in 9-mo-old 5XFAD mice following two *i.p.* injections (Fig. 1, C and D). In the acute treatment group, we also measured soluble TREM2 levels by ELISA and found an increase in soluble TREM2 in plasma and CSF in TREM2 antibody-treated groups compared to IgG control antibody-treated groups (Fig. 1, F and G). The meaning and interpretation of this increase is unclear, as the antibody binds to soluble TREM2 and may be prolonging its half-life. Following 3 mo of weekly *i.p.* injections of the TREM2 antibody in 5XFAD mice, there was increased clustering of activated CLEC7A⁺ microglia around A β plaques in the ipsilateral and contralateral cortex and HC of 5XFAD mice treated with the TREM2 antibody compared to mice treated with IgG control antibody (Fig. 1, H–K), suggesting that the TREM2 antibody increased TREM2 signaling in the brain. We also observed a non-statistically significant trend toward a decreased number of homeostatic P2RY12⁺ microglia around A β plaques in ipsilateral cortex and HC and the contralateral cortex (Fig. 1, L–O). Interestingly, when looking at total microglial cells using an Iba1 cellular stain, there was a significant increase in clustering and total number of cells around plaques in ipsilateral brain regions seeded with AD-tau (Fig. S1, A–D, G, H, K, and L). This effect of increased Iba1⁺ microglial cell clustering around A β plaques and increased total microglial cell percent area was not observed in the contralateral brain regions (Fig. S1, E, F, I, J, M, and N). These results are similar to those seen with another TREM2-activating antibody 4D9, where increased TREM2 and decreased P2RY12 expression was specifically observed in areas where microglia apparently clustered around amyloid plaques

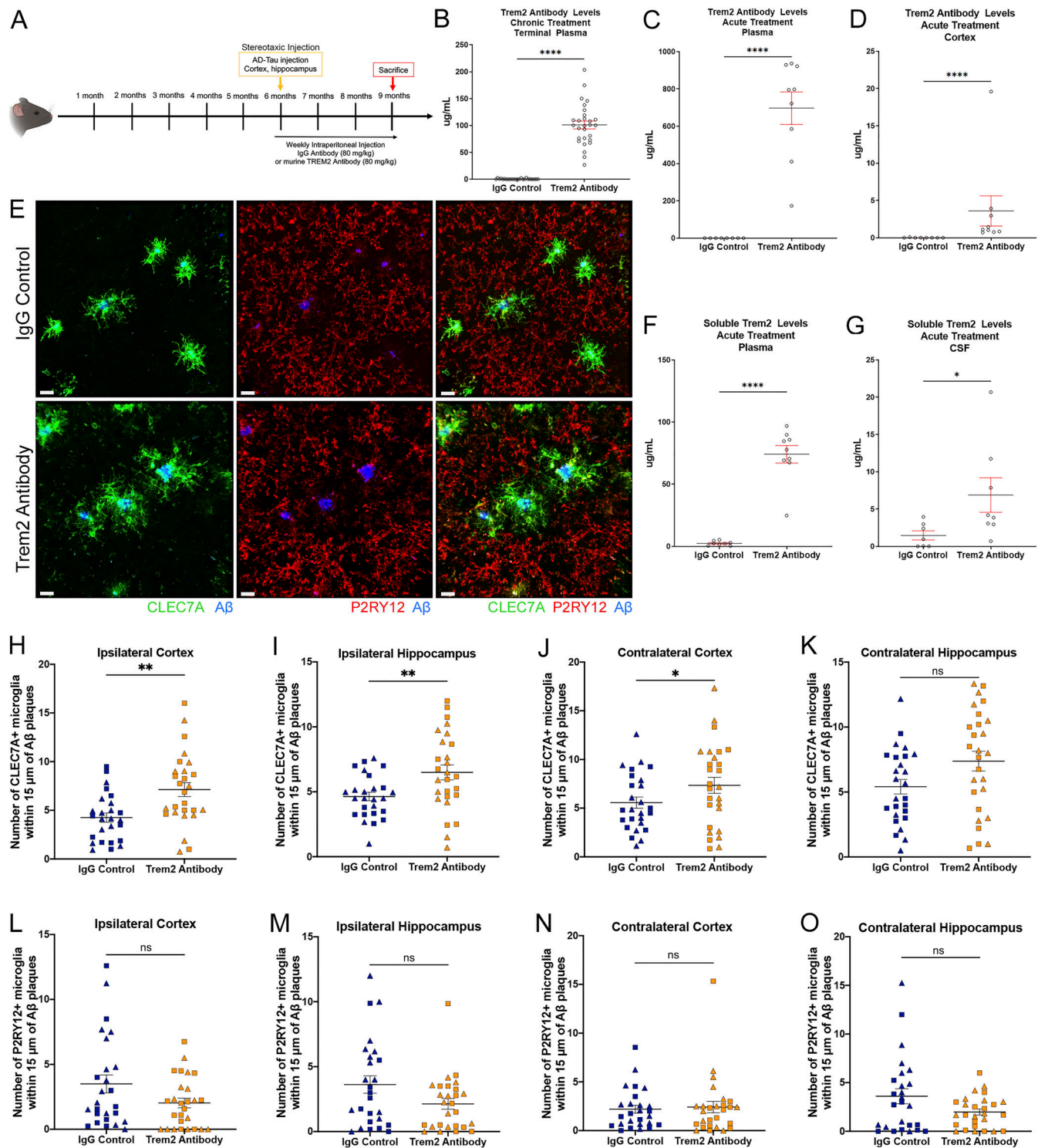


Figure 1. Chronic TREM2 activation increases DAM around plaques. (A) Schematic of experimental design. 6-mo-old 5XFAD mice were injected with AD-tau in the HC (bregma: -2.5 mm; lateral: -2.0 mm; depth: -2.2 mm) and overlying cortex (bregma: -2.5 mm; lateral: -2.0 mm; depth: -1.0 mm) and sacrificed 3 mo later to evaluate peri-plaque pathologies. 1 wk before AD-tau injection and every week following until sacrifice, 5XFAD mice were given i.p. injections of 80 mg/ml of the AL002a mouse TREM2 antibody ($n = 13$ female, $n = 14$ male) or the IgG control antibody ($n = 14$ female, $n = 12$ male). (B) Quantification of TREM2 antibody levels in terminal plasma for 5XFAD mice either chronically treated with the IgG control antibody or the TREM2 antibody. (C) Quantification of TREM2 antibody levels in plasma for 5XFAD mice either acutely treated with the IgG control antibody or the TREM2 antibody. (D) Quantification of TREM2 antibody levels in cortical tissue for 5XFAD mice either acutely treated with the IgG control antibody or the TREM2 antibody. For acute treatment, there were $n = 8$ IgG control and $n = 9$ Trem2 antibody-treated age- and sex-matched mice, unless otherwise specified on graphs. (E) Representative images of ipsilateral hemisphere stained with CLEC7A⁺ microglia, P2RY12⁺ microglia, and Aβ from IgG control and TREM2 antibody-treated groups. Scale bars, 15 μm. (F) Quantification of mouse sTREM2 levels in plasma for 5XFAD mice either acutely treated with the IgG control antibody or the TREM2 antibody. (G) Quantification

of TREM2 antibody levels in CSF for 5XFAD mice either acutely treated with the IgG control antibody or the TREM2 antibody. **(H–K)** Quantification of the number of CLEC7A⁺ microglia within 15 μ m of plaques in the ipsi- and contra- cortices (H and J) and hippocampi (I and K). **(L–O)** Quantification of the number of P2RY12⁺ microglia within 15 μ m of plaques in the ipsi- and contralateral cortices (L and N) and hippocampi (M and O). Triangle symbol represents female mice, and square symbol represents male mice. Data are presented as mean \pm SEM. Significance for B–D, F, and G was determined using a Mann-Whitney test and for H–O was determined using a linear regression with sex as a covariate. ns, $P > 0.05$; *, $P < 0.05$; **, $P < 0.01$; ***, $P < 0.001$.

with no overall changes seen in Iba1 numbers (Schlepckow et al., 2020). Loss of TREM2-mediated signaling inhibits the transition of microglia to a more DAM state characterized by enhanced migration, chemotaxis, and phagocytosis (Keren-Shaul et al., 2017; Mazaheri et al., 2017). We then investigated changes in other DAM markers CD68 and APOE in microglia around plaques after treatment with the TREM2 antibody. After treatment with the TREM2 antibody, the volume of CD68-positive puncta within microglia around plaques was significantly increased in the ipsilateral cortex and HC and the contralateral HC. We also observed a non-statistically significant trend towards increased CD68 puncta in microglia around plaques in the contralateral cortex (Fig. S3, A and C–F). Additionally, these findings were supported by significantly higher amounts of another DAM marker, ApoE, in the microglia around plaques in the TREM2 antibody treated groups vs. control IgG treated groups in the contralateral cortex and HC with trends toward increases in the ipsi-HC and ipsi-cortex (Fig. S3, B and G–J). These findings therefore suggest that chronic TREM2 activation through this antibody promotes the transition of the microglial cells to a more DAM-like state in proximity to A β plaques (Keren-Shaul et al., 2017; Krasemann et al., 2017; Mazaheri et al., 2017).

Chronic TREM2 agonist administration does not affect A β plaque burden and plaque conformation

Because TREM2 is critical for microglial clustering around plaques (Leyns et al., 2019; Wang et al., 2016; Yuan et al., 2016), we next investigated the impact of chronic TREM2 activation on A β plaques. In amyloid mouse models, studies have shown differing effects of TREM2 activation on A β plaque burden and plaque conformation. Peripheral injection of the anti-mouse TREM2 activating antibody AL002a has been shown to modestly decrease A β plaque deposition in 4-mo-old 5XFAD mice when there is early A β deposition in this model (Price et al., 2020). Additionally, an amyloid mouse model expressing human TREM2 treated with an anti-human TREM2 activating antibody AL002c reduced the number of filamentous plaques, increased the number of inert plaques, and had no change on the number of compact plaques (Wang et al., 2020). An acute treatment paradigm in 6-mo-old APP-NL-G-F mice demonstrated that an anti-mouse TREM2 activating antibody 4D9 reduced A β plaque load when measured with anti-A β antibody staining and soluble but not insoluble forms of A β 42 in the cortex of mice when detected through ELISA (Schlepckow et al., 2020). In our study, we first evaluated total A β plaque burden using an anti-A β antibody (HJ3.4). Following 3 mo of i.p. treatment with the TREM2 antibody, total A β plaque burden was not changed in male or female mice in the cortex or HC in either the ipsilateral or contralateral regions (Fig. 2, A–I). Next, we asked if there were changes in plaque conformation through staining X34⁺ fibrillar

plaques. We did not detect a change in plaque conformation and compaction after TREM2 antibody treatment in brain regions (Fig. S2, A–I). The fact that TREM2 antibody treatment did not decrease A β deposition could potentially be explained through the use of 6-mo-old 5XFAD mice, which already show robust A β plaque load at the start of our chronic treatment paradigm, an amount similar to that found in symptomatic individuals with AD. Most of the prior studies using mice with brain amyloid that showed effects of TREM2 antibodies on A β plaque burden and pathology studied younger animals with much less A β burden.

Chronic TREM2 agonist administration increases NP-tau pathology

We next investigated whether TREM2 antibody treatment impacts A β -induced NP-tau seeding and spreading. Unexpectedly, there was increased seeded NP-tau in the ipsilateral cortex and HC of 5XFAD male and female mice treated with the TREM2 antibody compared to mice treated with IgG control (Fig. 3, A–C, F, and G). There was also higher spreading of NP-tau pathology into the contralateral cortex of male mice (Fig. 3 H). There was no significant change in spreading of NP-tau pathology into the contralateral hemisphere of female mice and the contralateral HC of male mice (Fig. 4, D, E, and I). These results contrast with our previous studies that demonstrated TREM2 function impeded NP-tau seeding and spreading in the APPPS1-21 and 5XFAD amyloid mouse models expressing normal levels of TREM2 vs. mice with TREM2 deficiency (TREM2 knockout or TREM2 R47H knock-in mice) or following removal of microglia (Gratuze et al., 2021; Leyns et al., 2019). An important distinction between our prior (Leyns et al., 2019) vs. the current study is the germline KO or deficiency of TREM2 throughout life vs. the pharmacologic/biological manipulation of TREM2 after 6 mo of age in amyloid mice. Overall, this suggests that chronically agonizing TREM2 concomitant with induction of AD-tau seeding into the brain exacerbates A β -mediated tau seeding and to a certain extent spreading.

Chronic TREM2 agonist antibody administration increases peri-plaque NP-tau pathology, neuritic dystrophy, and loss of peri-plaque synaptic puncta

To confirm that cortical NP-tau pathology was increased after the TREM2 antibody treatment independently of the number of A β plaques, we performed confocal analysis and quantified the amount of NP-tau surrounding individual X34⁺ A β plaques. We confirmed on a per-plaque level that NP-tau pathology that represents seeding was increased in the ipsilateral HC of the TREM2 antibody treated mice (Fig. 4, B and H). We did not see a significant difference in the ipsilateral cortex and contralateral regions of our mice, possibly due to lower extent of seeding and spreading NP-tau levels in those regions (Fig. 4, G, I, and J).

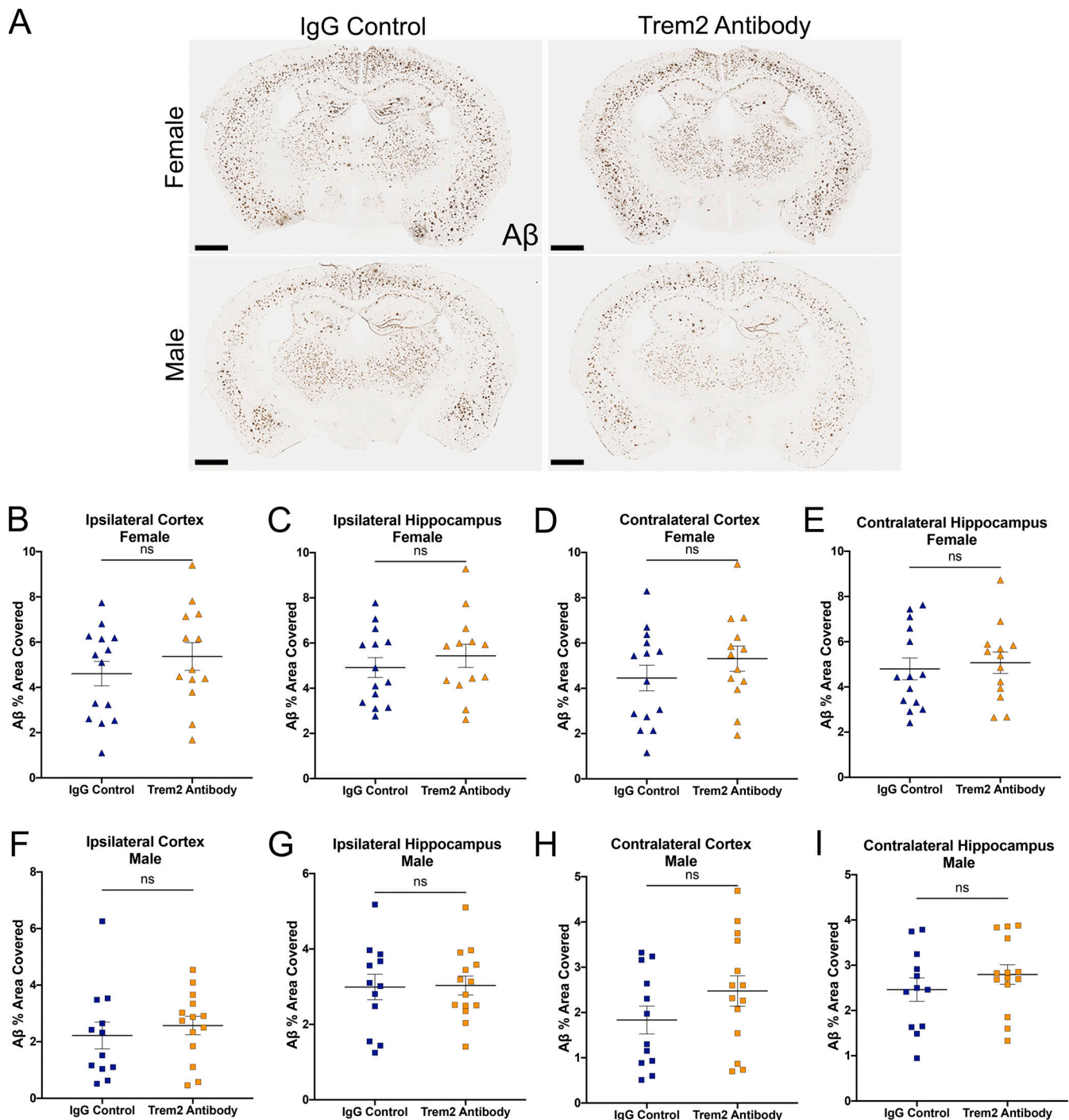


Figure 2. Chronic TREM2 activation with a TREM2 antibody results in no changes in A β plaque burden. (A) Representative images of A β plaques in 5XFAD mice either treated with the IgG control antibody or the TREM2 antibody. Scale bar, 100 μ m. (B–E) Quantification of A β staining in the ipsi- and contralateral cortices (B and D) and hippocampi (C and E) in female mice. (F–I) Quantification of A β staining in the ipsi- and contralateral cortices (F and H) and hippocampi (G and I) in male mice. Triangle symbol represents female mice, and square symbol represents male mice either treated with the IgG control antibody ($n = 14$ female, $n = 12$ male) or the TREM2 antibody ($n = 13$ female, $n = 14$ male). Data are presented as mean \pm SEM. Scale bar, 100 μ m. Significance was determined using a Student's *t* test. ns, $P > 0.05$.

TREM2 deficiency is associated with increased amyloid-dependent neuritic dystrophy, which in turn correlates with increased NP-tau seeding and spreading (Leyns et al., 2019). Thus, we next investigated the effect of the TREM2 antibody treatment on neuritic dystrophy around individual X34⁺ A β

plaques. In the ipsilateral cortex and HC, there was increased BACE1⁺ neuritic dystrophy around A β plaques in the TREM2 antibody treated mice (Fig. 4, A, C, and D). This effect was not seen in the contralateral brain regions (Fig. 4, E and F). These results contrast with the acute effects of the human TREM2-

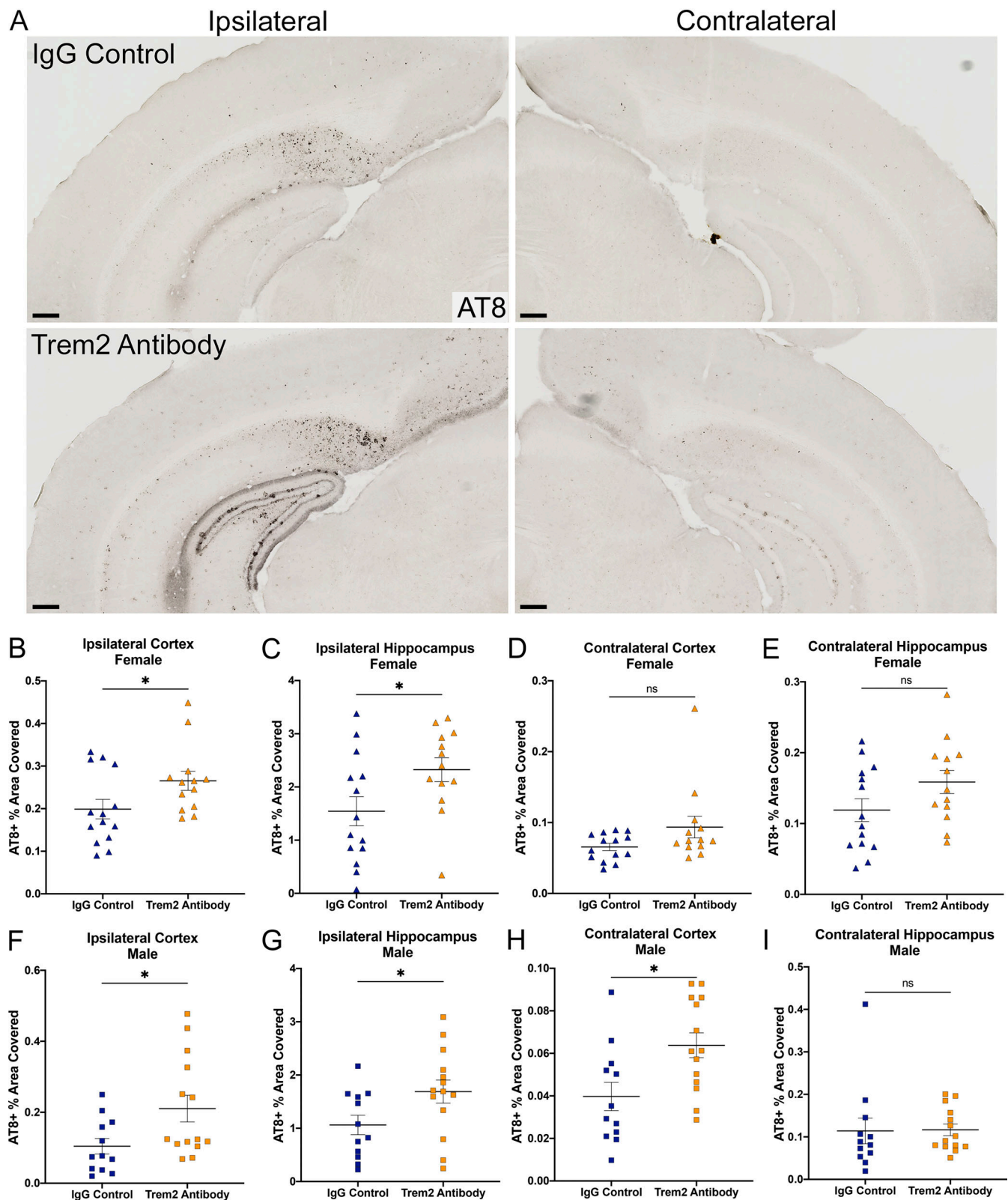


Figure 3. Chronic TREM2 activation with a TREM2 antibody increases NP-tau pathology. (A) Representative images of ipsi- and contralateral hemispheres stained with AT8+ NP-tau pathology in AD-tau injected 5XFAD mice either treated with the IgG control antibody or the TREM2 antibody. Representative images are from female mice. Scale bars, 100 μ m. (B–E) Quantification of p-tau (AT8+) staining in the ipsi- and contralateral cortices (B and D) and hippocampi (C and E) in female mice. (F–I) Quantification of p-tau (AT8+) staining in the ipsi- and contralateral cortices (F and H) and hippocampi (G and I) in male mice. Triangle symbol represents female mice, and square symbol represents male mice either treated with the IgG control antibody ($n = 14$ female, $n = 12$ male) or the TREM2 antibody ($n = 13$ female, $n = 14$ male). Data are presented as mean \pm SEM. Significance was determined using a Student's t test. ns, $P > 0.05$; *, $P < 0.05$.

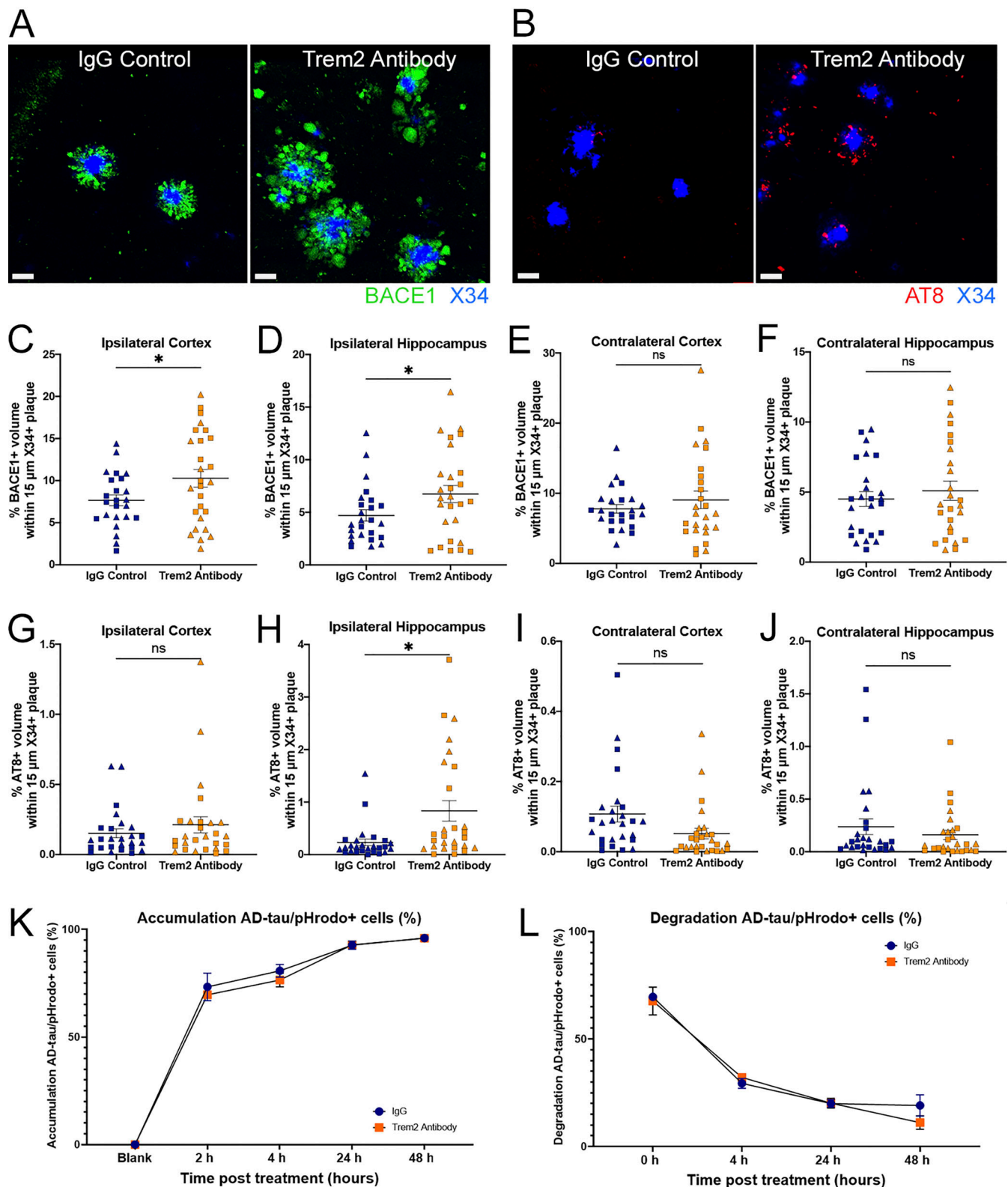


Figure 4. **Chronic TREM2 activation with a TREM2 antibody increases peri-plaque NP-tau pathology and plaque-associated neuritic dystrophy, and acute TREM2 activation results in no changes in AD-tau uptake and degradation.** (A) Representative images of BACE1⁺ and X34⁺ staining in ipsilateral HC. Scale bars, 20 μ m. (B) Representative images of AT8⁺ and X34⁺ staining in ipsilateral HC. (C–F) Quantification of the number of BACE1⁺ staining within 15 μ m of plaques in the ipsi- and contra- cortices (C and E) and hippocampi (D and F). (G–J) Quantification of the number of AT8⁺ staining within 15 μ m of plaques in the ipsi- and contra- cortices (G and I) and hippocampi (H and J). (K) AD-tau uptake assay in TREM2 WT BMDMs. Results represent two independent experiments. (L) AD-tau degradation assay in TREM2 WT BMDMs. Results represent two independent experiments. Triangle symbol represents female mice, and square symbol represents male mice either treated with the IgG control antibody ($n = 14$ female, $n = 12$ male) or the TREM2 antibody ($n = 13$ female, $n = 14$ male).

activating antibody studies using an amyloid model, where APP⁺ neurite coverage was significantly decreased in mice treated with the anti-human TREM2 antibody AL002c compared to control IgG (Wang et al., 2020). While the antibodies used in these studies are different, the reason for differing results are not clear.

Interestingly, we saw that the TREM2 agonistic antibody increased overall AT8-positive staining in both ipsilateral and contralateral HC and cortex while there was only enhanced NP-tau pathology on a per plaque level most significantly in the ipsilateral HC. The analysis for NP-associated tau pathology was within a 15-micron diameter around plaques. The NP-associated tau pathology can potentially occur beyond this border; however, there is also a possibility that TREM2 agonism may affect AT8-positive tau not associated with amyloid. Further studies will need to be conducted to investigate the effect of a TREM2 agonistic antibody on AT8-positive tau distinct from amyloid deposits.

We then asked if there were changes in the pre-synaptic marker synapsin around plaques following TREM2 antibody treatment. Interestingly, in the TREM2 antibody treatment group, we found greater loss of synapsin around plaques in the ipsilateral HC (Fig. 5, A and B). There were no significant changes in synapsin staining around plaques in the ipsilateral cortex and contralateral regions of the brain (Fig. 5, C-E). Overall, regions with higher levels of neuritic dystrophy and AT8⁺ tau pathology also displayed greater decreases of the pre-synaptic marker synapsin around plaques.

TREM2 acute activation does not affect AD-tau phagocytosis or degradation in bone marrow-derived macrophages (BMDMs)

Since we observed increased NP-tau seeding in the brains of mice treated with the TREM2 antibody compared to IgG control antibody, we tested the effect of TREM2 on the uptake and degradation of human AD-tau using an in vitro BMDMs phagocytosis assay through conjugating AD-tau with pHrodo. We have previously shown that there is no difference in AD-tau uptake between BMDMs cultured from TREM2 WT or TREM2 KO mice. However, we saw delayed AD-tau degradation in TREM2 KO BMDMs compared to TREM2 WT BMDMs (Gratuze et al., 2021). Following a 3-h pre-treatment with 10 μ g/ml of the Trem2 antibody or IgG control antibody, an increase in p-syk was found in the TREM2 antibody treated cells indicating increased TREM2 signaling compared to controls (Fig. S3 K). Despite the increase in TREM2 signaling, BMDMs from TREM2 WT mice demonstrated no differences in AD-tau uptake. We then asked whether the TREM2 antibody affected AD-tau degradation in BMDMs from TREM2 WT mice. We found that the TREM2 antibody did not change AD-tau degradation compared to the IgG control antibody in BMDMs from TREM2 WT mice. These results suggest that in contrast to acute pharmacological stimulation of TREM2, chronically agonizing TREM2 with an anti-

TREM2 antibody leads to an increase in A β -associated dystrophic neurites that appear to provide a better substrate for tau seeding and spreading (Fig. 4, A-J).

Conclusions

Until now, no studies have evaluated the role of chronic stimulation of TREM2 with a TREM2-activating antibody in the context of both A β and tau pathologies in adult mice with substantial amyloid pathology comparable to that seen in AD patients. Here, we investigated the role of TREM2 activation with an anti-TREM2 antibody on A β -induced tau seeding and spreading. A β pathology begins to develop about 20 yr before the onset of cognitive decline and plateaus just after cognitive decline begins in AD (Long and Holtzman, 2019). This is followed by the accumulation and spread of tau pathology in the neocortex. The location and amount of tau pathology correlates with clinical progression. For these reasons, how A β augments tau pathology to drive AD pathogenesis is a critical step in disease progression and needs to be better understood.

We employed a model of combined A β and tau pathology to investigate how manipulating microglial responses to A β pathology might affect the A β -induced onset and spread of tau pathology. Although we observed that chronic TREM2 activation increased the number of DAM clustering around A β plaques, surprisingly we found that chronic TREM2 activation increased seeding of NP-tau pathology in dystrophic neurons surrounding A β plaques, as well as to a certain extent the spreading of tau pathology compared to an IgG control treatment. This strong increase in NP-tau seeding is seen in both male and female mice and both ipsilateral cortex and HC. Additionally, we show that TREM2 activation increased loss of the pre-synaptic marker synapsin around plaques in the ipsilateral HC, the region having highest changes in NP-tau pathology and neuritic dystrophy.

Acutely, we show no differences in AD-tau uptake or degradation with the TREM2 antibody stimulation in BMDM cultures compared to an IgG control antibody. Our data suggest that during the phase of AD when A β is driving tau seeding and spreading, augmenting TREM2 activation with a TREM2 antibody in the absence of amyloid removal stimulates the microglial DAM phenotype and somehow increases tau seeding/spreading. Results from this study emphasize the fact that microglial function is context and disease-stage dependent. It is also important to note that not all TREM2 agonist antibodies are the same and whether they would all show the same effects is not clear. Further studies will need to be done to better understand how this transition to a DAM phenotype over a prolonged time without substantial changes in amyloid burden may contribute to increased tau pathology. Another important unanswered question within this line of studies is the effect of TREM2 agonist antibodies on amyloid-independent tau pathology. Likewise, more studies are essential for our understanding of how potential antagonism of TREM2 may affect amyloid induced tau seeding and spreading.

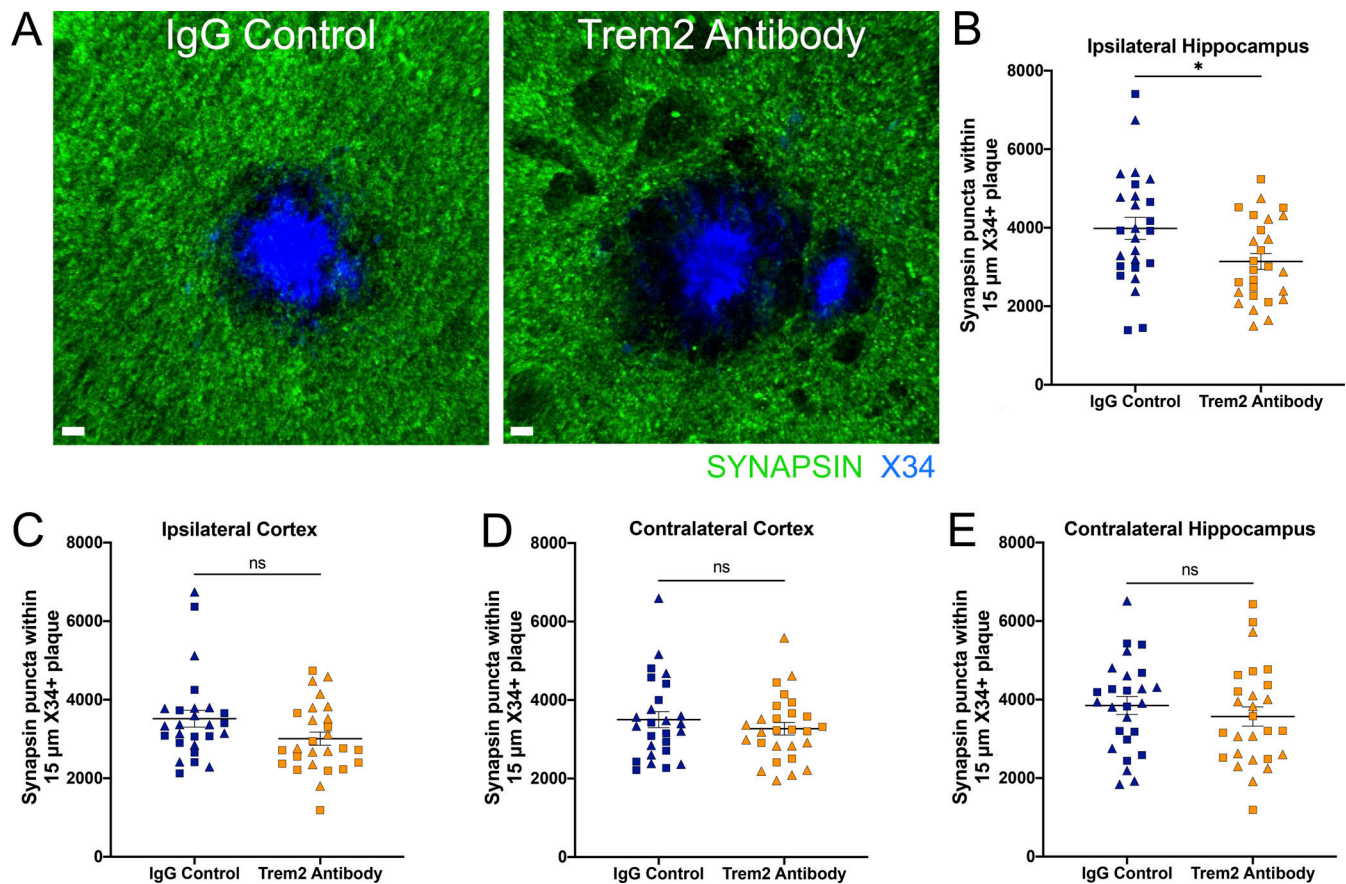


Figure 5. Chronic TREM2 activation with a TREM2 antibody increases peri-plaque loss of synaptic marker synapsin. (A) Representative images of Synapsin⁺ and X34⁺ staining in ipsilateral HC. Scale bar, 7 μ m. (B) Quantification of the number of Synapsin⁺ puncta within 15 μ m of plaques in the ipsi-HC. (C–E) Quantification of the number of Synapsin⁺ puncta within 15 μ m of plaques in the ipsi-cortex, contra-cortex, and HC. Triangle symbol represents female mice, and square symbol represents male mice either treated with the IgG control antibody ($n = 14$ female, $n = 12$ male) or the TREM2 antibody ($n = 13$ female, $n = 14$ male). Data are presented as mean \pm SEM. Significance was determined using a linear regression with sex as a covariate. ns, $P > 0.05$; *, $P < 0.05$.

Overall, our study provides immediate caveats on the best timepoint(s) on which TREM2 activation with TREM2 antibodies may be useful during the course of AD in humans. It suggests that it will be important to determine in human clinical trials whether chronically increasing TREM2 activation in people with mild cognitive impairment/very mild dementia who already have substantial amyloid deposition and where A β -induced tau seeding/spreading has already started will have beneficial vs. deleterious effects.

Materials and methods

Mice

5XFAD mice (Oakley et al., 2006) overexpressing both mutant human A β precursor protein with the Swedish (K670N and M671L), Florida (I716V), and London (V717I) familial AD mutations and human PS1 harboring two familial AD mutations, M146L and L286V, both under the control of the Thy1 promoter, were generated from mice purchased originally through The Jackson Laboratory (MMRRC; stock no. 34848; JAX). Male and female mice were utilized in this study. All mice were bred on a C57BL/6 background and housed in pathogen-free conditions

under a normal 12-h light/dark cycle. All animal protocols were approved by the Animals Studies Committee at Washington University in St. Louis School of Medicine.

Preparation of AD-tau aggregates from human AD brain tissue

AD-tau was isolated as previously described (Guo et al., 2016) from two human AD-brains. Using a bicinchoninic acid assay (catalog no. 23225; Thermo Fisher Scientific), the total protein concentration of the AD-tau preparation was 10.85 mg/ml. Tau-specific sandwich ELISA was used to determine the tau concentration in the preparation as previously described (Guo et al., 2016), which was found to be 5.0 μ g/ μ l. Prior to injection, AD-tau was diluted to a final concentration of 0.4 μ g/ μ l prior to injections and sonicated in a water bath sonicator (Q700; QSonica) for 30 s at 65% amplitude at 4°C.

Stereotactic intracerebral injections

6-mo-old 5XFAD mice were anesthetized with isoflurane, immobilized in a stereotactic frame (David Kopf Instruments), and unilaterally injected with 2 μ g AD-tau (1 μ g and a total of 2.5 μ l at each injection site) in the dentate gyrus (bregma: -2.5 mm; lateral: -2.0 mm; depth: -2.2 mm) and overlying cortex

(bregma: -2.5 mm; lateral: -2.0 mm; depth: -1.0 mm) using a Hamilton syringe (Hamilton; syringe: 80265-1702RNR; needle: 7803-07, type 4, 1.5 inches needle length, 60° angle). Mice were allowed to recover on a 37°C heating pad and monitored for the first 72 h after surgery.

Brain extraction and preparation

Mice were anesthetized by i.p. injection of pentobarbital (200 mg/kg). Blood samples were collected in EDTA-treated tubes prior to a cardiac perfusion with 3 U/ml heparin in cold Dulbecco's PBS. Blood samples were spun for at 4°C for 10 min at 2,000 *g* and top layer of blood plasma was collected. For the 9-month-old AD-tau-injected 5XFAD mice, whole brains were carefully extracted and fixed in 4% paraformaldehyde for 48 h before being transferring to 30% sucrose and stored at 4°C until they were sectioned. Brains were cut coronally into 30 μ m sections on a freezing sliding microtome (HM 400; Microm) and stored in cryoprotectant solution (0.2 M PBS, 15% sucrose, and 33% ethylene glycol) at -20°C until use. A small nick was placed on the left hemisphere at the piriform cortex with a clean razor blade to ensure identification of the ipsilateral injected side.

Immunohistochemistry (IHC) and immunofluorescence (IF)

For IHC staining of NP-tau (AT8, mouse monoclonal, 1:500; catalog no. MN1020B; Thermo Fisher Scientific) and A β (HJ3.4 biotinylated, anti-A β 1-13, mouse monoclonal, 2 μ g/ml generated in house), sections were washed three times in TBS for 5 min and blocked in 0.3% hydrogen peroxide for 15 min. After washing, sections were blocked in 3% milk in TBS with 0.25% Triton X-100 for 30 min. Primary antibody was diluted in 3% milk/Triton X-100, and the sections were incubated in the primary antibody overnight at 4°C. The next day, sections were washed three times. For AT8 and HJ3.4 staining, after washing, sections were incubated in ABC Elite solution (PK-6100; VectaStain) for 1 h, prepared following the manufacturer's instructions, followed by another washing step. Sections were developed in 3,3'-diaminobenzidine solution (catalog no. SK4103; Vector Laboratories for Iba1; catalog no. D5905; Sigma-Aldrich for AT8 and HJ3.4), washed, and mounted on slides. After drying overnight, the slides were dehydrated in increasing ethanol concentrations followed by xylene and coverslipped using Cytoseal 60 (catalog no. 8310; Thermo Fisher Scientific).

For IF staining, co-stains were performed for (1) X34, BACE1, AT8, and Iba1; and (2) A β , Clec7a, P2RY12, and Iba1. Fibrillar A β was stained by X34 dye (SML-1954, 1:3,000; Sigma-Aldrich), BACE1 (catalog no. ab108394, 1:500; Abcam), AT8 (MN1020B, 1:500; Thermo Fisher Scientific), Iba1 (catalog no. ab5076, 1:500; Abcam), A β (HJ3.4 biotinylated, generated in-house, 2 μ g/ml), Clec7a (catalog no. mabg-mdect, 1:100; InvivoGen), P2RY12 (gift from Dr. Oleg Butovsky, 1:1,000), Synapsin-1/2 (catalog no. 106004, 1:500; Synaptic systems), CD68 (catalog no. MCA1957, 1:500; AbD SeroTec) and ApoE (HJ6.3 biotinylated, generated in-house, 1:300) were used to evaluate peri plaque pathologies.

Free-floating sections were washed three times in PBS for 5 min each and then permeabilized in 0.25% Triton X-100 PBS (PBS-X) for 30 min. Tissue sections were then incubated in X34 for 20 min, washed in X34 buffer (40% EtOH in PBS), and

washed in PBS twice. Sections were incubated in blocking solution for 30 min (3% BSA, 3% normal donkey serum, and 0.1% PBS-X) before incubating in primary antibodies in blocking solution overnight at 4°C. The next day, sections were washed three times in PBS for 5 min each, placed in secondary antibodies for 2 h (Thermo Fisher Scientific; 1:500) at room temperature (RT), and then washed three times in PBS for 20 min each. Lipofuscin was quenched with 0.1% Sudan black through a 10 min incubation and washed once in 0.02% PBS-Tween 20 for 5 min and then in PBS for 5 min. Sections were mounted, sealed in Fluoromount-G (catalog no. 0100-01; SouthernBiotech), and stored in the dark at 4°C until imaging. For synapsin staining, free-floating tissue were blocked in 20% normal goat serum (NGS) in PBS for 1 h at RT. Tissues were then incubated overnight at RT with primary antibodies in 10% NGS containing 0.3% PBS-X. The following day, sections were rinsed three times, 5 min each, in PBS followed by incubation in secondary antibodies in 10% NGS containing 0.3% PBS-X for 4 h at RT. Sections were mounted, dried at RT, briefly rinsed in distilled water, and then coverslipped. Mounting medium was prepared the day of use by mixing Tris-MWL 4-88 (17977-150; Electron Microscopy Sciences) with AF300 (17977-25; Electron Microscopy Sciences) at a 9:1 ratio.

Image acquisition and analysis

Images were obtained from three to four sections per mouse for IHC and two to three sections per mouse for IF. For IHC stains, slides were scanned on the NanoZoomer 2.0-HT system (Hamamatsu Photonics). Images were further processed using NDP viewing software (Hamamatsu Photonics) and Fiji software version 2.1.0 (National Institutes of Health). For IF images, four to six z-stacks (20 μ m) per section were acquired on an LSM 880 II Airyscan FAST confocal microscope (Zeiss) with a 20 \times objective, 2 \times zoom, and 1,024 \times 1,024 resolution. IF images for synapses were acquired on a Leica Stellaris 5 confocal microscope with a 63 \times objective and 1,024 \times 1,024 resolution.

Quantification of confocal images for AT8 volume, BACE1 volume, ApoE, and CD68 around X34⁺ or HJ3.4⁺ plaques was performed on a semiautomated platform using MATLAB and Imaris 9.5 software (Bitplane). To create surfaces of each stain based on a threshold applied to all images, X34⁺ or HJ3.4⁺ surfaces were dilated by 15 μ m and colocalized with various immunostained surfaces. For quantification of the number of plaque-associated Iba1⁺, Clec7a⁺, P2RY12⁺ microglia, and Synapsin⁺ puncta, a threshold was applied across all images to assign spots to each cell body or puncta. X34 or HJ3.4⁺ surfaces were dilated 15 μ m, and spots were counted within the X34⁺ or HJ3.4⁺ dilated surface. All staining experiments were imaged and quantified by a blinded investigator. GraphPad Prism was utilized to generate data plots.

BMDM culture and in vitro phagocytosis assay

BMDMs were differentiated from bone marrow cells isolated from WT mice in BMDM differentiation media (RPMI 1640 medium, 10% FBS, 10% L929 supernatant, 1 \times Pen-Strep, 1 \times Glutamax, 1 \times sodium pyruvate, and 1 \times nonessential amino acids) for 4–5 d depending on confluence. When fully differentiated

BMDMs were 70% confluent, non-tissue culture-treated 96-well plates were seeded with 30,000 cells in BMDM media for a phagocytosis/degradation assay the next day. To assess for Syk phosphorylation through Western blot analysis, a subset of cells was treated with either IgG control antibody or TREM2 antibody (10 µg/ml) that was directly added to the media for 3 h.

All AD-tau phagocytosis or degradation assays were conducted with prepared cell culture as described above. Prior to each assay, wells were incubated with either the TREM2 antibody or an IgG control antibody for 3 h at a concentration of 10 µg/ml. AD-tau conjugated with pH-sensitive pHrodo red dye was added into each well at final concentration of 50 nM at 48, 24, 4, 2, and 0 h before harvesting cells. For degradation assay, all cells were treated with AD-tau for 1 h and switched to normal media for 0, 4, 24, and 48 h before being harvested. After washing with PBS twice, BMDMs were resuspended with MACS buffer (PBS, 1 mM EDTA, and 0.5% BSA), and flow cytometry was performed on a BD LSRFortessa flow cytometer at the flow cytometry core at Washington University in St. Louis. pHrodo signal was determined by the PE yellow laser after gating with for live singlet BMDM cells and further analyzed by FlowJo.

Acute TREM2 antibody treatment for TREM2 p-Syk and Syk activation assessment, TREM2 antibody level assessment and soluble TREM2 level assessment

9-mo-old 5XFAD mice were given two i.p. injections at 7 d apart with 80 mg/kg of the murine TREM2 antibody or with 80 mg/kg of a murine IgG control antibody. On day 8, mice were anesthetized by i.p. injection of pentobarbital (200 mg/kg). CSF, cortical tissue, and plasma were collected for protein and antibody level analysis.

Assessment of p-Syk and Syk levels in BMDMs and cortical lysates

Analysis of p-Syk and Syk levels were performed on 20 µg of total protein from samples processed in SDS-loading buffer and boiled for 10 min. Samples were loaded on a 4–20% Mini-PROTEAN gel (catalog no. 4561094; Bio-Rad) and transferred onto a polyvinylidene fluoride membrane. Membranes were blocked in 5% BSA-TBS with 0.02% Tween-20 for 1 h and incubated in primary antibody diluted (catalog no. 2710, 1:1,000; Cell Signaling; catalog no. 13198, 1:1,000; Cell Signaling) in 5% BSA-TBS with 0.02% Tween-20 overnight shaking at 4°C. The next day, after washing, secondary antibodies were applied for 1 h, shaking at RT. Membrane was washed three times for 5 min, developed using Pierce ECL Western Blotting Substrate (catalog no. 32106; Thermo Fisher Scientific), and imaged using a ChemiDoc imaging system. Blots were converted to grayscale and densitometry analysis was performed in ImageJ. Photoshop was used for post-quantification editing. Original unedited blots are available in the source data file for Fig. S3.

TREM2 antibody measurements in plasma and CSF

IgG levels in the plasma were measured using a custom TREM2 IgG MSD assay. Briefly, single spot MSD plates (Meso Scale Discovery) were coated with 25 µl/well of 2 µg/ml recombinant mouse TREM2 protein in PBS overnight at 4°C. Plates were then

washed (PBS + 0.05% Tween-20) and blocked with binding buffer (PBS + 3% BSA) for at least 1 h at RT. Samples were titrated in binding buffer, added to the plate at 50 µl/well, and incubated for 1 h at RT with shaking. Plates were washed again. Anti-TREM2 antibodies were detected using a goat anti-mouse sulfo tag conjugated secondary antibody (Meso Scale Discovery). Plates were washed. 150 µl 1× Read buffer was added and plates were analyzed on a Sector Imager (Meso Scale Discovery).

Mouse soluble TREM2 ELISA

A custom ELISA was developed to measure soluble TREM2 levels in the plasma and TREM2 levels in the brain lysates. The ELISA was successfully validated using supernatant from TREM2 WT vs. KO BMDMs. Briefly, the bin 3 anti-TREM2 antibody ADI-9 was captured on a high-binding ELISA plate at 1 µg/ml in PBS overnight at 4°C. The plates were washed three times using PBS/0.05% Triton. As a standard, 156–10,000 pg/ml mouse TREM2-Fc (R&D Systems) was added to the plates, as well as diluted plasma or brain samples in binding buffer (PBS + 1% BSA). Plates containing samples and standard were incubated at RT for 1 h. The plates were washed three times using PBS/0.05% Triton. Biotinylated rat anti-TREM2 antibody (R&D Systems) was added at 1:10,000 dilution in binding buffer and incubated for 1 h at RT. The plates were washed three times using PBS/0.05% Triton. Streptavidin-HRP (1:200 in binding buffer, R&D Systems) was added to the plates and incubated for 20–30 min at RT. The plates were washed three times using PBS/0.05% Triton. TMB substrate solution was added and incubated until color developed. The reaction was stopped by adding 50 µl of 2 N sulfuric acid and the plate was read in a Synergy H1 plate reader at 450 and 630 nm.

Statistics

Data were analyzed using GraphPad Prism v.9 or R v4.1.1 and presented as the mean ± SEM (*, $P < 0.05$; **, $P < 0.01$; and ***, $P < 0.0001$). For comparisons of two groups, unpaired *t* test was used. Linear models on R were utilized to adjust for sex as a covariate in comparisons. All samples or animals were included in the statistical analysis unless otherwise specified.

Online supplemental material

Fig. S1 shows that chronic TREM2 activation increases microgliosis and microglial clustering in ipsilateral brain regions. Fig. S2 shows that chronic TREM2 activation does not change fibrillar plaque conformation. Fig. S3 shows that chronic TREM2 activation results in an increase in the expression of CD68 and ApoE in microglia around plaques and that treatment with the Trem2 antibody increase syk activation in BMDMs and mouse cortical brain tissue.

Acknowledgments

The AL002a antibody and IgG control antibody were provided by Alector.

Confocal data were supported by the Office of Research Infrastructure, a part of the National Institutes of Health Office of the Director (OD021629), the Washington University School of Medicine (CDI-CORE-2015-505 and CDI-CORE-2019-813), the

Children's Discovery Institute of Washington University and St. Louis Children's Hospital, and the Foundation for Barnes-Jewish Hospital (3770 and 4642). This study was supported by grants from the National Institutes of Health (AG047644 to D.M. Holtzman) and the JPB Foundation (D.M. Holtzman).

Author contributions: N. Jain, J.D. Ulrich, and D.M. Holtzman designed the study. N. Jain performed the experiments and analyzed the data. C.A. Lewis assisted in microscopy of periplaque synapsin and apoE analysis. N. Jain, J.D. Ulrich, and D.M. Holtzman wrote the manuscript. All authors discussed the results and commented on the manuscript.

Disclosures: J.D. Ulrich and D.M. Holtzman reported a patent to anti-TREM2 agonist antibodies pending. D.M. Holtzman reported "other" from C2N Diagnostics, Genentech, Denali, Cajal Neurosciences, and Alector outside the submitted work. No other disclosures were reported.

Submitted: 13 April 2022

Revised: 26 July 2022

Accepted: 8 September 2022

References

- Atagi, Y., C.C. Liu, M.M. Painter, X.F. Chen, C. Verbeeck, H. Zheng, X. Li, R. Rademakers, S.S. Kang, H. Xu, et al. 2015. Apolipoprotein E is a ligand for triggering receptor expressed on myeloid cells 2 (TREM2). *J. Biol. Chem.* 290:26043–26050. <https://doi.org/10.1074/jbc.M115.679043>
- Butovsky, O., and H.L. Weiner. 2018. Microglial signatures and their role in health and disease. *Nat. Rev. Neurosci.* 19:622–635. <https://doi.org/10.1038/s41583-018-0057-5>
- Cheng, Q., J. Danao, S. Talreja, P. Wen, J. Yin, N. Sun, C.M. Li, D. Chui, D. Tran, S. Koirala, et al. 2018. TREM2-activating antibodies abrogate the negative pleiotropic effects of the Alzheimer's disease variant Trem2R47H on murine myeloid cell function. *J. Biol. Chem.* 293:12620–12633. <https://doi.org/10.1074/jbc.RA118.001848>
- Cignarella, F., F. Filippello, B. Bollman, C. Cantoni, A. Locca, R. Mikesell, M. Manis, A. Ibrahim, L. Deng, B.A. Benitez, et al. 2020. TREM2 activation on microglia promotes myelin debris clearance and remyelination in a model of multiple sclerosis. *Acta Neuropathol.* 140:513–534. <https://doi.org/10.1007/s00401-020-02193-z>
- Colonna, M., and Y. Wang. 2016. TREM2 variants: New keys to decipher Alzheimer disease pathogenesis. *Nat. Rev. Neurosci.* 17:201–207. <https://doi.org/10.1038/nrn.2016.7>
- Cui, X., J. Qiao, S. Liu, M. Wu, and W. Gu. 2021. Mechanism of TREM2/DAP12 complex affecting β -amyloid plaque deposition in Alzheimer's disease modeled mice through mediating inflammatory response. *Brain Res. Bull.* 166:21–28. <https://doi.org/10.1016/j.brainresbull.2020.10.006>
- Deczkowska, A., H. Keren-Shaul, A. Weiner, M. Colonna, M. Schwartz, and I. Amit. 2018. Disease-associated microglia: A universal immune sensor of neurodegeneration. *Cell.* 173:1073–1081. <https://doi.org/10.1016/j.cell.2018.05.003>
- Domingues, H.S., C.C. Portugal, R. Socodato, and J.B. Relvas. 2016. Oligodendrocyte, astrocyte, and microglia crosstalk in myelin development, damage, and repair. *Front. Cell Dev. Biol.* 4:71. <https://doi.org/10.3389/fcell.2016.00071>
- Ellwanger, D.C., S. Wang, S. Brioschi, Z. Shao, L. Green, R. Case, D. Yoo, D. Weishuhn, P. Rathanaswami, J. Bradley, et al. 2021. Prior activation state shapes the microglia response to antihuman TREM2 in a mouse model of Alzheimer's disease. *Proc. Natl. Acad. Sci. USA.* 118:e2017742118. <https://doi.org/10.1073/PNAS.2017742118>
- Fassler, M., M.S. Rappaport, C.B. Cuño, and J. George. 2021. Engagement of TREM2 by a novel monoclonal antibody induces activation of microglia and improves cognitive function in Alzheimer's disease models. *J. Neuroinflammation.* 18:19. <https://doi.org/10.1186/s12974-020-01980-5>
- Ginhoux, F., and M. Williams. 2016. Tissue-resident macrophage ontogeny and homeostasis. *Immunity.* 44:439–449. <https://doi.org/10.1016/j.immuni.2016.02.024>
- Gratuze, M., Y. Chen, S. Parhizkar, N. Jain, M.R. Strickland, J.R. Serrano, M. Colonna, J.D. Ulrich, and D.M. Holtzman. 2021. Activated microglia mitigate A β -associated tau seeding and spreading. *J. Exp. Med.* 218: e20210542. <https://doi.org/10.1084/jem.20210542>
- Gratuze, M., C.E.G. Leyns, and D.M. Holtzman. 2018. New insights into the role of TREM2 in Alzheimer's disease. *Mol. Neurodegener.* 13:66. <https://doi.org/10.1186/s13024-018-0298-9>
- Gratuze, M., C.E. Leyns, A.D. Sauerbeck, M.K. St-Pierre, M. Xiong, N. Kim, J.R. Serrano, M.E. Tremblay, T.T. Kummer, M. Colonna, et al. 2020. Impact of TREM2R47H variant on tau pathology-induced gliosis and neurodegeneration. *J. Clin. Invest.* 130:4954–4968. <https://doi.org/10.1172/JCI138179>
- Guerreiro, R., A. Wojtas, J. Bras, M. Carrasquillo, E. Rogava, E. Majounie, C. Cruchaga, C. Sassi, J.S.K. Kauwe, S. Younkin, et al. 2013. TREM2 variants in Alzheimer's disease. *N. Engl. J. Med.* 368:117–127. <https://doi.org/10.1056/nejmoa1211851>
- Guo, J.L., S. Narasimhan, L. Changolkar, Z. He, A. Stieber, B. Zhang, R.J. Gathagan, M. Iba, J.D. McBride, J.Q. Trojanowski, and V.M.Y. Lee. 2016. Unique pathological tau conformers from Alzheimer's brains transmit tau pathology in nontransgenic mice. *J. Exp. Med.* 213:2635–2654. <https://doi.org/10.1084/jem.20160833>
- He, Z., J.L. Guo, J.D. McBride, S. Narasimhan, H. Kim, L. Changolkar, B. Zhang, R.J. Gathagan, C. Yue, C. Dengler, et al. 2018. Amyloid- β plaques enhance Alzheimer's brain tau-seeded pathologies by facilitating neuritic plaque tau aggregation. *Nat. Med.* 24:29–38. <https://doi.org/10.1038/nm.4443>
- Holtzman, D.M., J.C. Morris, & A.M. Goate. 2011. Alzheimer's disease: The challenge of the second century. *Sci. Transl. Med.* 3:77sr1. <https://doi.org/10.1126/scitranslmed.3002369>
- Jonsson, T., H. Stefansson, S. Steinberg, I. Jonsson, P.v. Jonsson, J. Snaedal, S. Bjornsson, J. Huttenlocher, A.I. Levey, J.J. Lah, et al. 2013. Variant of TREM2 associated with the risk of Alzheimer's disease. *N. Engl. J. Med.* 368:107–116. <https://doi.org/10.1056/nejmoa1211103>
- Keren-Shaul, H., A. Spinrad, A. Weiner, O. Matcovitch-Natan, R. Dvir-Szternfeld, T.K. Ulland, E. David, K. Baruch, D. Lara-Astaiso, B. Toth, et al. 2017. A unique microglia type Associated with restricting development of Alzheimer's disease. *Cell.* 169:1276–1290.e17. <https://doi.org/10.1016/j.cell.2017.05.018>
- Krasemann, S., C. Madore, R. Cialic, C. Baufeld, N. Calcagno, R. el Fatimy, L. Beckers, E. O'Loughlin, Y. Xu, Z. Fanek, et al. 2017. The TREM2-APOE pathway drives the transcriptional phenotype of dysfunctional microglia in neurodegenerative diseases. *Immunity.* 47:566–581.e9. <https://doi.org/10.1016/j.immuni.2017.08.008>
- Lanier, L.L., B. Corliss, J. Wu, and J.H. Phillips. 1998. Association of DAP12 with activating CD94/NKG2C NK cell receptors. *Immunity.* 8:693–701. [https://doi.org/10.1016/S1074-7613\(00\)80574-9](https://doi.org/10.1016/S1074-7613(00)80574-9)
- Leyns, C.E.G., M. Gratuze, S. Narasimhan, N. Jain, L.J. Koscal, H. Jiang, M. Manis, M. Colonna, V.M.Y. Lee, J.D. Ulrich, and D.M. Holtzman. 2019. TREM2 function impedes tau seeding in neuritic plaques. *Nat. Neurosci.* 22:1217–1222. <https://doi.org/10.1038/s41593-019-0433-0>
- Leyns, C.E.G., J.D. Ulrich, M.B. Finn, F.R. Stewart, L.J. Koscal, J. Serrano, G.O. Robinson, E. Anderson, M. Colonna, and D.M. Holtzman. 2017. TREM2 deficiency attenuates neuroinflammation and protects against neurodegeneration in a mouse model of tauopathy. *Proc. Natl. Acad. Sci. USA.* 114:11524–11529. <https://doi.org/10.1073/pnas.1710311114>
- Long, J.M., and D.M. Holtzman. 2019. Alzheimer disease: An update on pathobiology and treatment strategies. *Cell.* 179:312–339. <https://doi.org/10.1016/j.cell.2019.09.001>
- Mazaheri, F., N. Snaidero, G. Kleinberger, C. Madore, A. Daria, G. Werner, S. Krasemann, A. Capell, D. Trümbach, W. Wurst, et al. 2017. TREM2 deficiency impairs chemotaxis and microglial responses to neuronal injury. *EMBO Rep.* 18:1186–1198. <https://doi.org/10.15252/embr.201743922>
- Nelson, P.T., I. Alafuzoff, E.H. Bigio, C. Bouras, H. Braak, N.J. Cairns, R.J. Castellani, B.J. Crain, P. Davies, K. Del Tredici, et al. 2012. Correlation of alzheimer disease neuropathologic changes with cognitive status: A review of the literature. *J. Neuropathol. Exp. Neurol.* 71:362–381. <https://doi.org/10.1097/NEN.0b013e31825018f7>
- Netea, M.G., J. Domínguez-Andrés, L.B. Barreiro, T. Chavakis, M. Divangahi, E. Fuchs, L.A.B. Joosten, J.W.M. van der Meer, M.M. Mhlanga, W.J.M. Mulder, et al. 2020. Defining trained immunity and its role in health and disease. *Nat. Rev. Immunol.* 20:375–388. <https://doi.org/10.1038/s41577-020-0285-6>
- Nugent, A.A., K. Lin, B. van Lengerich, S. Lianoglou, L. Przybyla, S.S. Davis, C. Llapashtica, J. Wang, D.J. Kim, D. Xia, et al. 2020. TREM2 regulates

- microglial cholesterol metabolism upon chronic phagocytic challenge. *Neuron*. 105:837–854.e9. <https://doi.org/10.1016/j.neuron.2019.12.007>
- Oakley, H., S.L. Cole, S. Logan, E. Maus, P. Shao, J. Craft, A. Guillozet-Bongaerts, M. Ohno, J. Disterhoft, L. van Eldik, et al. 2006. Intraneuronal beta-amyloid aggregates, neurodegeneration, and neuron loss in transgenic mice with five familial Alzheimer's disease mutations: Potential factors in amyloid plaque formation. *J. Neurosci.* 26:10129–10140. <https://doi.org/10.1523/JNEUROSCI.1202-06.2006>
- Price, B.R., T.L. Sudduth, E.M. Weekman, S. Johnson, D. Hawthorne, A. Woolums, and D.M. Wilcock. 2020. Therapeutic Trem2 activation ameliorates amyloid-beta deposition and improves cognition in the 5XFAD model of amyloid deposition. *J. Neuroinflammation*. 17:238. <https://doi.org/10.1186/s12974-020-01915-0>
- Ransohoff, R.M. 2016. How neuroinflammation contributes to neurodegeneration. *Science*. 353:777–783. <https://doi.org/10.1126/science.aag2590>
- Ruan, Z., D. Pathak, S. Venkatesan Kalavai, A. Yoshii-Kitahara, S. Muraoka, N. Bhatt, K. Takamatsu-Yukawa, J. Hu, Y. Wang, S. Hersch, et al. 2021. Alzheimer's disease brain-derived extracellular vesicles spread tau pathology in interneurons. *Brain*. 144:288–309. <https://doi.org/10.1093/brain/awaa376>
- Schlepckow, K., K.M. Monroe, G. Kleinberger, L. Cantuti-Castelvetri, S. Parhizkar, D. Xia, M. Willem, G. Werner, N. Pettkus, B. Brunner, et al. 2020. Enhancing protective microglial activities with a dual function TREM 2 antibody to the stalk region. *EMBO Mol. Med.* 12:e11227. <https://doi.org/10.15252/emmm.201911227>
- Ulland, T.K., W.M. Song, S.C. Huang, J.D. Ulrich, A. Sergushichev, W.L. Beatty, A.A. Loboda, Y. Zhou, N.J. Cairns, A. Kambal, et al. 2017. TREM2 maintains microglial metabolic fitness in Alzheimer's disease. *Cell*. 170: 649–663.e13. <https://doi.org/10.1016/j.cell.2017.07.023>
- Ulrich, J.D., T.K. Ulland, M. Colonna, and D.M. Holtzman. 2017. Elucidating the role of TREM2 in Alzheimer's disease. *Neuron*. 94:237–248. <https://doi.org/10.1016/j.neuron.2017.02.042>
- Wang, S., M. Mustafa, C.M. Yuede, S.V. Salazar, P. Kong, H. Long, M. Ward, O. Siddiqui, R. Paul, S. Gilfillan, et al. 2020. Anti-human TREM2 induces microglia proliferation and reduces pathology in an Alzheimer's disease model. *J. Exp. Med.* 217:e20200785. <https://doi.org/10.1084/jem.20200785>
- Wang, Y., M. Cella, K. Mallinson, J.D. Ulrich, K.L. Young, M.L. Robinette, S. Gilfillan, G.M. Krishnan, S. Sudhakar, B.H. Zinselmeyer, et al. 2015. TREM2 lipid sensing sustains the microglial response in an Alzheimer's disease model. *Cell*. 160:1061–1071. <https://doi.org/10.1016/j.cell.2015.01.049>
- Wang, Y., T.K. Ulland, J.D. Ulrich, W. Song, J.A. Tzaferis, J.T. Hole, P. Yuan, T.E. Mahan, Y. Shi, S. Gilfillan, et al. 2016. TREM2-mediated early microglial response limits diffusion and toxicity of amyloid plaques. *J. Exp. Med.* 213:667–675. <https://doi.org/10.1084/jem.20151948>
- Yuan, P., C. Condello, C.D. Keene, Y. Wang, T.D. Bird, S.M. Paul, W. Luo, M. Colonna, D. Baddeley, and J. Grutzendler. 2016. TREM2 haploinsufficiency in mice and humans impairs the microglia barrier function leading to decreased amyloid compaction and severe axonal dystrophy. *Neuron*. 90:724–739. <https://doi.org/10.1016/j.neuron.2016.05.003>

Supplemental material

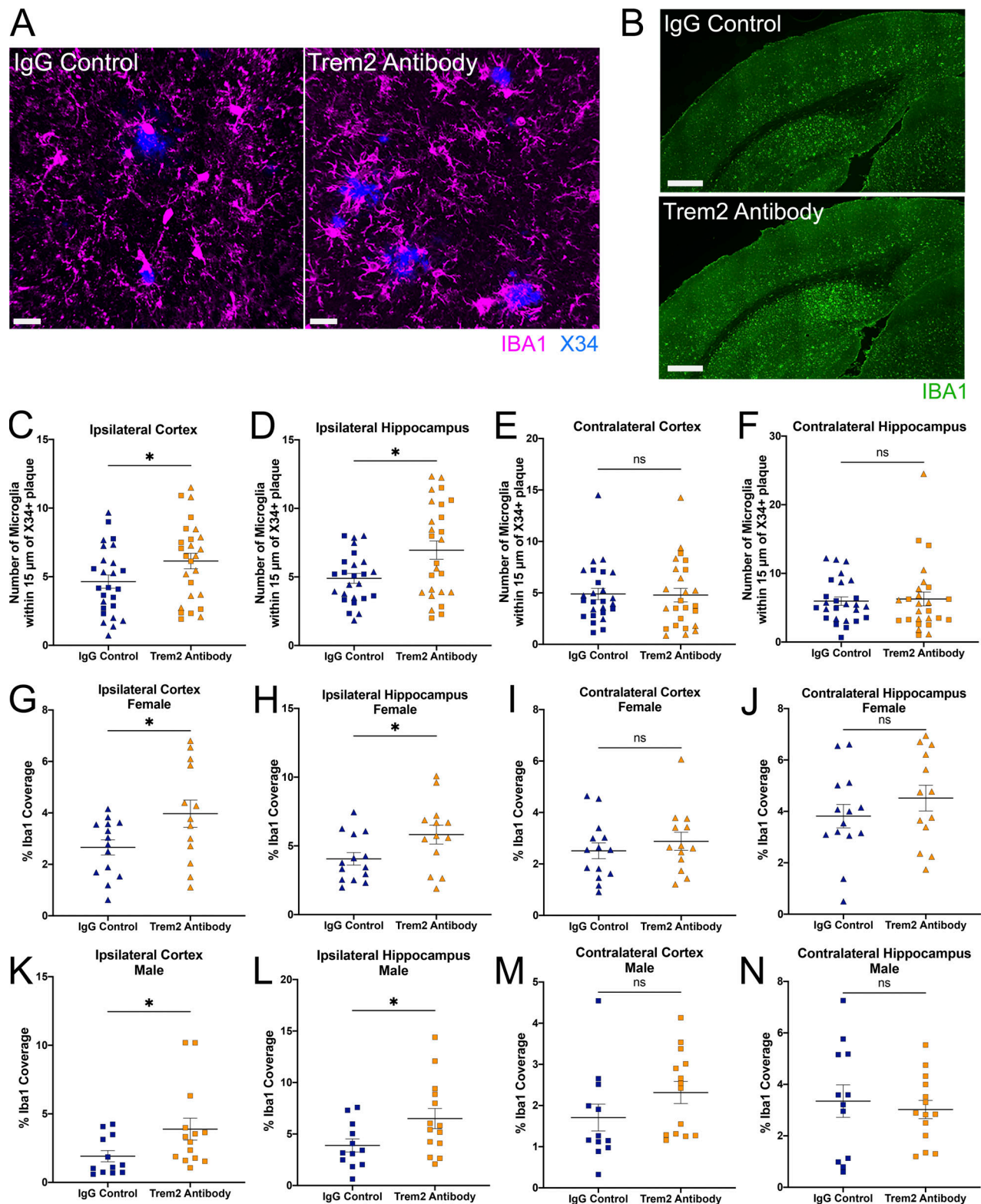


Figure S1. Chronic TREM2 activation with a TREM2 antibody increases microgliosis and microglial clustering in ipsilateral brain regions. (A) Representative images of ipsilateral hemispheres stained with Iba1⁺ microglia and X34⁺ fibrillar plaques. Scale bars, 20 μ m. (B) Representative images of ipsilateral hemispheres stained with Iba1⁺ microglia. Scale bars, 100 μ m. (C–F) Quantification of the number of Iba1⁺ microglia within 15 μ m of plaques in the ipsi- and contra- cortices and hippocampi. (G–J) Quantification of total percent area of Iba1⁺ staining in the ipsi- and contralateral cortices (G and I) and hippocampi (H and J) in female mice. Triangle symbol represents female mice, and square symbol represents male mice either treated with the IgG control antibody ($n = 14$ female, $n = 12$ male) or the TREM2 antibody ($n = 13$ female, $n = 14$ male). Data are presented as mean \pm SEM. Significance for C and D was determined using a linear regression with sex as a covariate and for G–N using a Student's t test. ns, $P > 0.05$; *, $P < 0.05$.

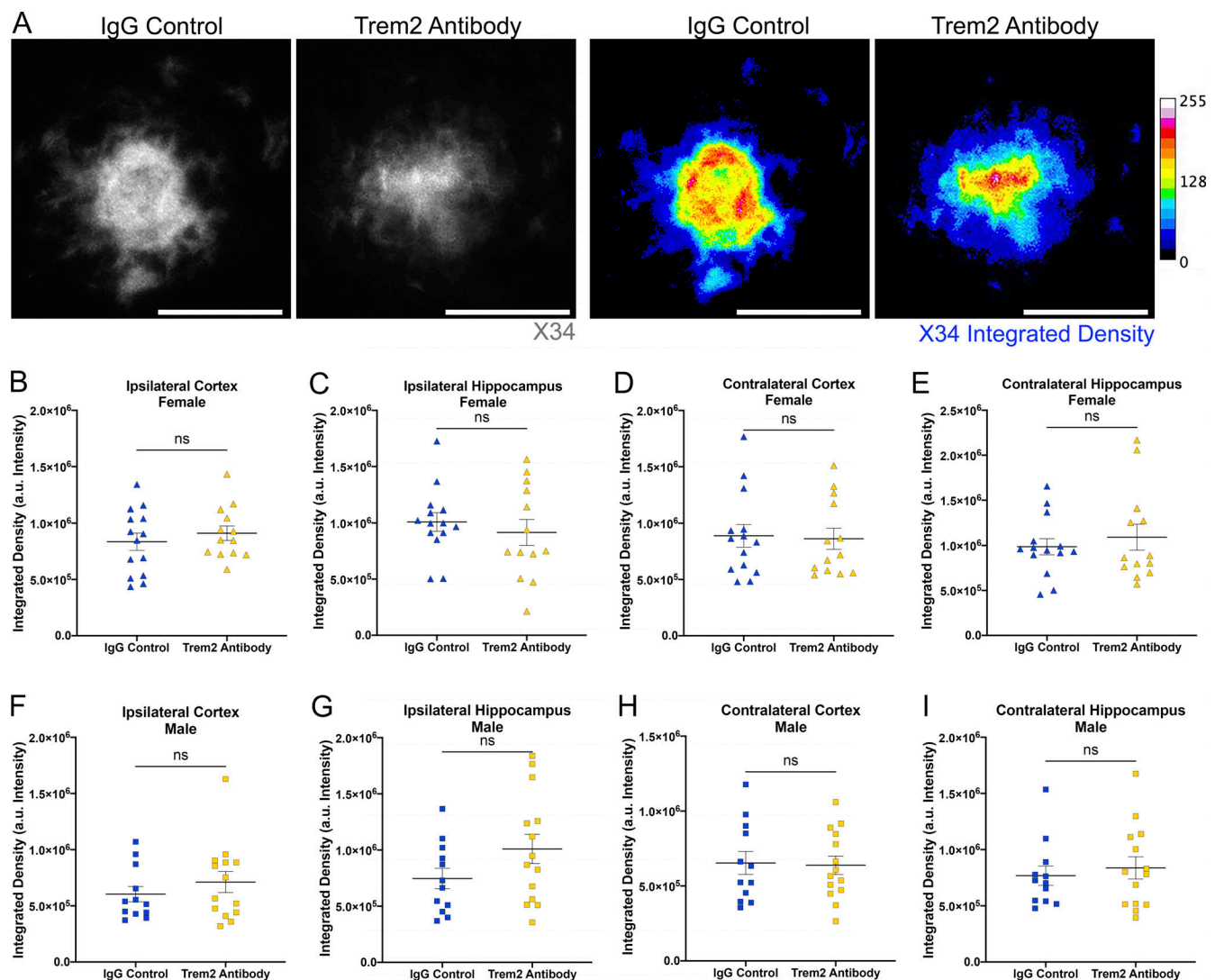


Figure S2. **Chronic TREM2 activation with a TREM2 antibody does not change fibrillar plaque conformation.** (A) Representative images of X34⁺ plaque conformation in grayscale and heat-density map based on intensity (red is equivalent to highest intensity, and blue is lowest intensity) for 5XFAD mice either treated with the IgG control antibody or the TREM2 antibody. Scale bar, 20 μ m. (B–E) Quantification of X34⁺ integrated density intensity measurements in the ipsi- and contralateral cortices (B and D) and hippocampi (C and E) in female mice. (F–I) Quantification of X34⁺ integrated density intensity measurements in the ipsi- and contralateral cortices (B and D) and hippocampi (C and E) in male mice. Triangle symbol represents female mice, and square symbol represents male mice either treated with the IgG control antibody ($n = 14$ female, $n = 12$ male) or the TREM2 antibody ($n = 13$ female, $n = 14$ male). Data are presented as mean \pm SEM. Significance was determined using a Student's t test. ns, $P > 0.05$.

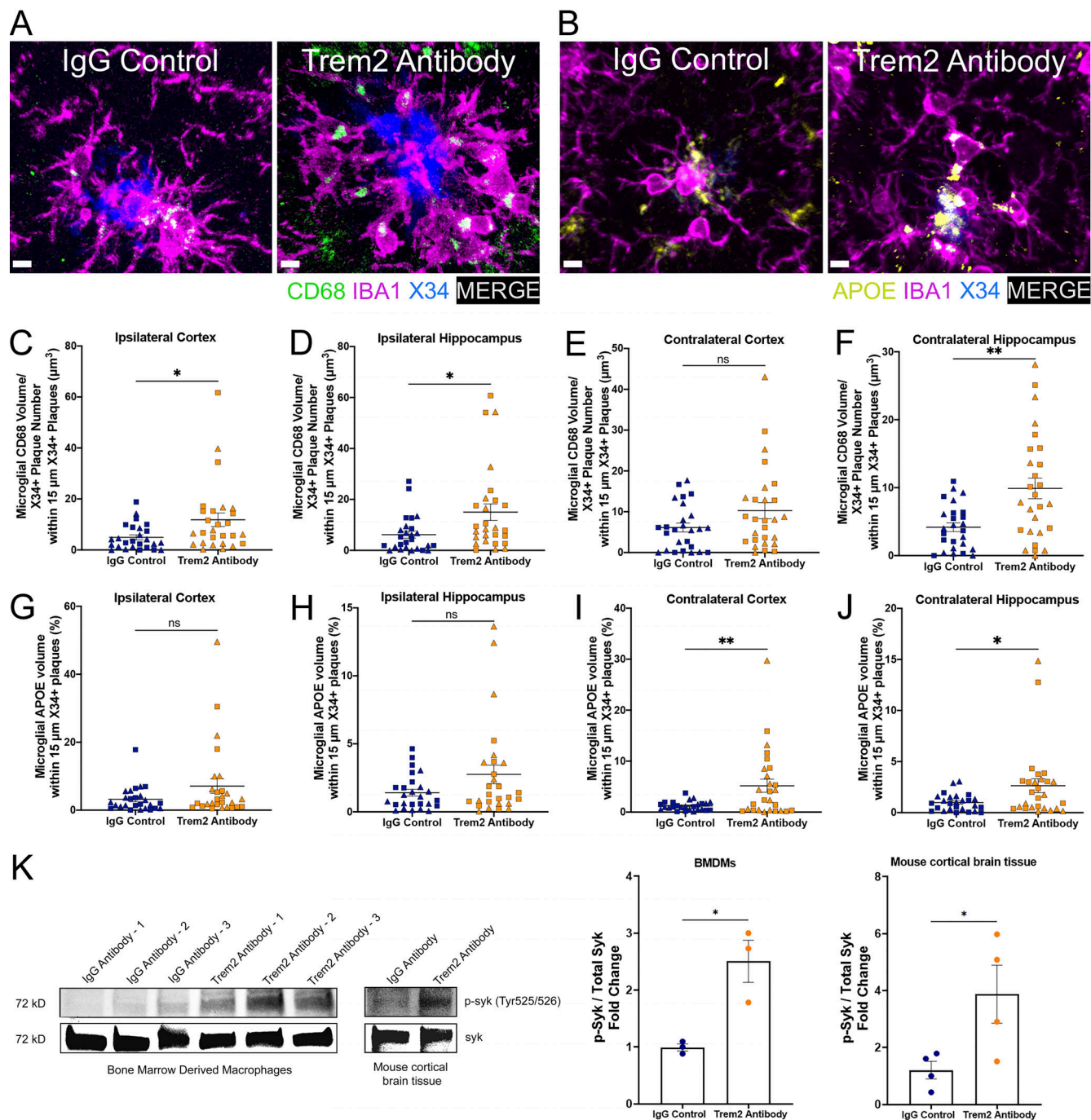


Figure S3. Chronic TREM2 activation with a TREM2 antibody increases peri-plaque microglial CD68 and ApoE and syk signaling. (A) Representative images of CD68⁺ puncta, IBA1⁺, and X34⁺ staining in ipsilateral HC. Scale bar, 5 μ m. (B) Representative images of APOE⁺, IBA1⁺, and X34⁺ staining in ipsilateral HC. (C–F) Quantification of the number of microglial CD68⁺ staining within 15 μ m of plaques in the ipsi- and contra- cortices (C and E) and hippocampi (D and F). (G–J) Quantification of the number of microglial ApoE⁺ staining within 15 μ m of plaques in the ipsi- and contra- cortices (G and I) and hippocampi (H and J). (K) Western blot analysis of p-syk normalized to total syk of BMDMs treated with IgG control antibody or Trem2 antibody. Immunoblot analysis of p-syk and syk protein levels in BMDMs and in mouse cortical brain tissue. Unedited blots are included in source data. In C–J, triangle symbol represents female mice, and square symbol represents male mice either treated with the IgG control antibody ($n = 14$ female, $n = 12$ male) or the TREM2 antibody ($n = 13$ female, $n = 14$ male). Data are presented as mean \pm SEM. Significance for C–J was determined using a linear regression with sex as a covariate. Significance for K was determined using a Student's t test. ns, $P > 0.05$; *, $P < 0.05$; **, $P < 0.01$. Source data are available for this figure: SourceData FS3.